Encapsulation of benznidazole in nanostructured lipid carriers and increased trypanocidal activity in a resistant *Trypanosoma cruzi* strain

Flávia Lidiane Oliveira da Silva[1], Maria Betânia de Freitas Marques[1,2],
Maria Irene Yoshida[2], Wagner da Nova Mussel[2],
João Vinícios Wirbitzki da Silveira[3], Poliana Ribeiro Barroso[1],
Kelly Cristina Kato[1], Helen Rodrigues Martins[1], Guilherme Carneiro[1*]

[1]Department of Pharmacy, Faculty of Biological and Health Sciences, Federal University
of Jequitinhonha and Mucuri Valleys, Diamantina, Minas Gerais, Brazil, [2]Department
of Chemistry, Institute of Exact Sciences, Federal University of Minas Gerais, Belo
Horizonte, Minas Gerais, Brazil, [3]Institute of Science and Technology, Federal University
of Jequitinhonha and Mucuri Valleys, Diamantina, Minas Gerais, Brazil

Chagas disease is a neglected parasitic disease caused by *Trypanosoma cruzi*, whose treatment has remained unsatisfactory for over 50 years, given that it is limited to two drugs. Benznidazole (BZN) is an efficient antichagasic drug used as the first choice, although its poor water-solubility, irregular oral absorption, low efficacy in the chronic phase, and various associated adverse effects are limiting factors for treatment. Incorporating drugs with such characteristics into nanostructured lipid carriers (NLC) is a promising alternative to overcome these limiting obstacles, enhancing drug efficacy and bioavailability while reducing toxicity. Therefore, this study proposed NLC-BZN formulations in different compositions prepared by hot-melt homogenization followed by ultrasound, and the optimized formulation was characterized by FTIR, DRX, DSC, and thermogravimetry. Biological activities included *in vitro* membrane toxicity (red blood cells), fibroblast cell cytotoxicity, and trypanocidal activity against epimastigotes of the Colombian strain of *T. cruzi*. The optimized NLC-BZN had a small size (110 nm), negative zeta potential (-18.0 mV), and high encapsulation (1.64% of drug loading), as shown by infrared spectroscopy, X-ray diffraction, and thermal analysis. The NLC-BZN also promoted lower *in vitro* membrane toxicity (<3% hemolysis), and 50% cytotoxic concentration (CC_{50}) for NLC-BZN in L929 fibroblast cells (110.7 µg/mL) was twice the value as the free BZN (51.3 µg/mL). Our findings showed that the NLC-BZN had higher trypanocidal activity than free BZN against the epimastigotes of the resistant Colombian strain, and this novel NLC-BZN formulation proved to be a promising tool in treating Chagas disease and considered suitable for oral and parenteral administration.

Keywords: Drug delivery systems. Lipid nanoparticles. Nanomedicine. Neglected diseases. Poorly water-soluble drugs. Thermal analysis.

INTRODUCTION

Chagas disease (CD) is an anthropozoonosis affecting millions of people; it is considered one of the most neglected tropical diseases and is estimated to be responsible for 12,000 deaths and 56,000 new cases yearly (WHO, 2020; PAHO, 2020). This condition is caused by the protozoan *Trypanosoma cruzi* and is characterized by two distinct clinical phases. The initial acute phase is associated with high parasitemia, lasting 4–8 weeks. The late chronic phase is characterized by the evolution of the disease to critical clinical manifestations in the heart or gastrointestinal tract, albeit with a remarkable

*Correspondence: G. Carneiro. Departamento de Farmácia. Faculdade de Ciências Biológicas e da Saúde. Universidade Federal dos Vales do Jequitinhonha e Mucuri. Rodovia MGT 367, Km 583. CEP 39100-000, Diamantina, MG, Brasil. E-mail: guilherme.carneiro@ufvjm.edu.br; guifafar@yahoo.com.br. Phone: +55 38 3532-1200 * 8865. Fax +55 38 35321249. ORCID: https://orcid.org/0000-0002-0367-8170

Flávia L. O. Silva, Maria B. F. Marques, Maria I. Yoshida, Wagner N. Mussel, João V. W. Silveira, Poliana R. Barroso, Kelly C. Kato, Helen R. Martins, Guilherme Carneiro

decrease in parasitemia. Some patients may even have an indeterminate form of CD and remain asymptomatic along these phases (Prata, 2001).

The condition of a neglected disease is clearly observed in the history of CD therapy, which has remained the same since the 1970s; it is restricted to only two drugs: nifurtimox (NFX) and benznidazole (BZN) (Romero, Morilla, 2010). Despite both drugs having parasitological cure rates above 70–80% in the acute phase, they are not efficient in the chronic phase (Morilla, Romero, 2015). Moreover, both BZN and NFX cause various adverse effects, usually leading to treatment discontinuation by the patients. As BZN shows better tolerability, a broader action spectrum, and higher tissue penetration, it is usually preferred over NFX and considered the first-choice drug in CD treatment, although researchers have reported resistance of *T. cruzi* strains to BZN (Maximiano *et al.*, 2010; Salomon, 2012; Perez-Molina, Molina, 2018).

Despite the main BZN dosage form being oral tablets, its low aqueous solubility (0.2–0.4 mg/mL) is the main drawback for oral administration (Lamas *et al.*, 2006; Maximiano *et al.*, 2010), leading to irregular absorption, variable pharmacokinetic profile, and low bioavailability (Maximiano *et al.*, 2011a). Thus, alternatives to increase the BZN solubility in the gastrointestinal tract have been proposed to achieve higher bioavailability and reduce adverse effects (Ferraz *et al.*, 2018). Among these strategies, there is complexation with cyclodextrins (Maximiano *et al.*, 2011a; Soares-Sobrinho *et al.*, 2011; Soares-Sobrinho *et al.*, 2012), the use of BZN microcrystals (Maximiano *et al.*, 2011b) and nanocrystals (Scalise *et al.*, 2016), solid dispersions (Lima *et al.*, 2011; Leonardi, Salomon, 2013; Palmeiro-Roldan *et al.*, 2014; Fonseca-Berzal *et al.*, 2015; Simonazzi *et al.*, 2018), incorporating BZN into chitosan microparticles (Leonardi *et al.*, 2009), calcium carbonate nanoparticles (Tessarolo *et al.*, 2018), and polymeric micro- and nanoparticles (Seremeta *et al.*, 2019).

Drug encapsulation in nanocarrier systems is an important strategy used to increase the solubility and bioavailability of many poorly water-soluble drugs, and incorporating BZN into lipid nanoparticles is a relevant field to be explored. Nanostructured lipid carriers (NLC) are the second generation of lipid nanoparticles, and the solid matrix consists of a mixture of solid and liquid lipids, where the drug molecules can be encapsulated. These nanocarriers have been successfully proposed to improve many therapies, such as cancer, heart and brain diseases, antibiotics, and even vaccines. The presence of oils makes the solid lipid matrix more unstructured and with more imperfections to accommodate higher quantities of the drug (Gaba *et al.*, 2015; Beloqui *et al.*, 2017). The high biocompatibility of the excipients in their composition is vital for safe drug use; at the same time, these nanosystems can provide other benefits for the BZN treatment, their high stability during storage, the potential for controlled drug release from the lipid matrix, enhanced oral absorption, and versatility in administration through different routes (Gaba *et al.*, 2015; Beloqui *et al.*, 2017).

Few efforts have been made to propose lipid nanocarriers for BZN incorporation in the form of liposomes (Morilla *et al.*, 2002; Vinuesa *et al.*, 2017), nanoemulsions (Streck *et al.*, 2014), microemulsions (Streck *et al.*, 2016), and even lipid nanoparticles (Vinuesa *et al.*, 2017). However, the efficiency of BZN incorporation in all these systems is low in terms of drug/lipid ratio, and high encapsulation has only been reached with high lipid amounts. Given the limited and unsatisfactory CD therapies available and the potential of NLC for high incorporation of poorly water-soluble drugs, this study sought to develop BZN-loaded NLCs with higher drug-loading capacity in low lipid amounts in order to address the cytotoxicity profile and *in vitro* trypanocidal activity of the optimized formulation.

MATERIAL AND METHODS

Material

Benznidazole (100.2% purity) was directly extracted from tablets (LAFEPE, Brazil), according to Branquinho *et al.* (2014). The NLC components were Compritol 888 ATO kindly provided by Gattefossé (Lyon, France) and Super Refined Tween 80 and Crodamol GTCC kindly provided by Croda Inc. (Edison, USA). Poloxamer 407 (Pluracare F127; Chemspecs, Brazil), egg lecithin (Lipoid

E 80; Lipoid GmbH, Germany), soy lecithin (Cargill, Germany), cholesterol (Sigma-Aldrich, USA), and glycerol (Isofar, Brazil) were also utilized as indicated. All other reagents and solvents used were of analytical or HPLC grade without further purification.

A 4% red blood cell (RBC) suspension kit (Bio-Rad, Brazil) and saponin (INLAB, Brazil) were utilized in the *in vitro* membrane toxicity studies. The *in vitro* cell culture studies employed 3-(4,5-dimethylthiazol-2yl)-2,5-diphenyltetrazolium bromide (MTT), RPMI 1640, L-glutamine, penicillin, streptomycin, hemin (Sigma-Aldrich, USA), fetal bovine serum (FBS; Gibco Life Technologies, USA), and liver infusion tryptose (LIT) medium (BD, USA).

Development of BZN lipid nanoparticles

As utilized in previous studies (Marcial, Carneiro, Leite, 2017; Fernandes *et al.*, 2018), the composition of the NLC matrix consisted of Compritol and Crodamol GTCC (medium chain triglycerides, MCT) as solid and liquid lipids, respectively. Surfactants were proposed alone or mixed: Tween 80 (TW80), egg lecithin (EL),

soy lecithin (SL), and poloxamer 407 (P407). Cholesterol (Chol) was utilized as a co-surfactant when present. The main goal at this stage was higher BZN incorporation with smaller and homogeneous particle sizes.

From the original NLC formulation (Marcial, Carneiro, Leite, 2017; Fernandes *et al.*, 2018) containing 0.05% (w/v) BZN, four screening studies were conducted (Table I). The first study was performed to verify the influence of liquid lipids. Thus, NLC A contained MCT, NLC B contained MCT + Chol, and NLC C contained soybean oil. The next study was the influence of the surfactant system, with the following mixtures in the composition: NLC D had TW80 + SL (1:1), NLC E had TW80 + EL (1:1), NLC F had TW80 + P407 (1:1), and NLC G had just P407. The third study involved variations in the lipid/surfactant ratio: 3:1 (NLC H), 3:2 (NLC I), 5:2 (NLC J), and 5:1 (NLC K). Lastly, BZN was incorporated into the optimized formulation in increasing amounts: 0.1 % (w/v) (NLC L) and 0.2 % (w/v) (NLC M). For further studies, the formulation considered optimized in the final analysis was named NLC-BZN, and the respective blank formulation (without BZN) was b-NLC.

TABLE I - Composition matrix (% w/w) and characterization of BZN-loaded NLC formulations (BZN concentration = 0.05% w/w): hydrodynamic diameter, polydispersity index (PDI), zeta potential (ZP), and encapsulation efficiency (EE).

Formulation	Lipids			Surfactant System					Characterization Parameters			
	Compritol	MCT	SO	TW80	P407	SL	EL	Chol	Diameter (nm)	PI	ZP (mV)	EE (%)
NLC A	1.2	0.3	-	1	-	-	-	-	114 ± 2	0.25 ± 0.02	-15.9 ± 1.3	83.0 ± 0.6
NLC B	1.2	-	0.3	1	-	-	-	-	114 ± 2	0.26 ± 0.01	-18.9 ± 1.0	74.5 ± 0.2*
NLC C	1.2	0.3	-	1	-	-	-	0.15	115 ± 1	0.26 ± 0.01	-26.4 ± 1.2*	74.2 ± 2.5*
NLC D	1.2	0.3	-	0.5	-	0.5	-	-	119 ± 2	0.29 ± 0.03	-46.0 ± 1.3*	72.0 ± 1.9*
NLC E	1.2	0.3	-	0.5	-	-	0.5	-	190 ± 2*	0.42 ± 0.01*	-30.2 ± 1.1*	83.9 ± 1.3
NLC F	1.2	0.3	-	0.5	0.5	-	-	-	110 ± 3	0.19 ± 0.01*	-18.0 ± 2.6	82.6 ± 2.1
NLC G	1.2	0.3	-	-	1	-	-	-	131 ± 2*	0.26 ± 0.04	-28.1 ± 1.0*	78.3 ± 0.7*
NLC H	2.4	0.6	-	0.5	0.5	-	-	-	191 ± 2**	0.21 ± 0.00	-16.0 ± 0.3	84.9 ± 0,2

Flávia L. O. Silva, Maria B. F. Marques, Maria I. Yoshida, Wagner N. Mussel, João V. W. Silveira, Poliana R. Barroso, Kelly C. Kato, Helen R. Martins, Guilherme Carneiro

TABLE I - Composition matrix (% w/w) and characterization of BZN-loaded NLC formulations (BZN concentration = 0.05% w/w): hydrodynamic diameter, polydispersity index (PDI), zeta potential (ZP), and encapsulation efficiency (EE).

Formulation	Lipids			Surfactant System					Characterization Parameters			
	Compritol	MCT	SO	TW80	P407	SL	EL	Chol	Diameter (nm)	PI	ZP (mV)	EE (%)
NLC I	2.4	0.6	-	1	1	-	-	-	147 ± 6**	0.23 ± 0.02**	-6.0 ± 0.6**	80.7 ± 0.8
NLC J	4	1	-	1	1	-	-	-	180 ± 3**	0.25 ± 0.01**	-32.0 ± 0.9**	80.7 ± 0.2
NLC K	4	1	-	0.5	0.5	-	-	-	330 ± 1**	0.25 ± 0.02**	-30.4 ± 0.9**	75.1 ± 0.3**

Abbreviations: MCT – medium chain triglycerides; SO – soybean oil; TW80 – Tween 80; SL – soybean lecithin; EL – egg lecithin; Chol – cholesterol. PI – polydispersion index; ZP – zeta potential; EE – encapsulation efficiency.

Lipids with amphipathic properties, such as SL, EL (phospholipids) and Chol (steroid) were considered included in the surfactant system.

[*] Represents significant difference in relation to NLC A ($p < 0.05$), n=3.

[**] Represents significant difference in relation to NLC F ($p < 0.05$), n =3.

Nanoparticle preparation

Formulations were prepared by the hot-melt homogenization method followed by ultrasonication, as reported elsewhere (Marcial, Carneiro, Leite, 2017). Briefly, the oily phase (OP) containing lipids and surfactants was heated at 85 °C and the aqueous phase (AP), a 2.25% (w/v) glycerol solution in water, was preheated at the same temperature (batch: 20 mL). When present, BZN was previously solubilized in the OP. Next, AP was slowly poured onto the OP, and the mixture was stirred for 2 min and immediately homogenized with a high-intensity ultrasonic probe (Q55 sonicator; Qsonica, Church Hill Road, Newton, USA) for 10 min (40% amplitude). The final pH was adjusted to 7.0.

Particle size and zeta potential

The average hydrodynamic diameter and zeta potential (ZP) were determined in a Zetasizer Nano ZS (Malvern Instruments; Worcestershire, England) at a 173° angle and 25 ºC. Formulations were 10-fold diluted in AP before the measurements. All determinations were performed in triplicate, and the maximum acceptable value to consider the sample monodisperse was a polydispersity index (PDI) of 0.3.

Drug encapsulation efficiency

The BZN quantification was performed using the HPLC method previously developed and validated (Almeida *et al.*, 2016). Encapsulation efficiency (EE) was determined from the quantification of BZN before (total BZN) and after filtration (filtered BZN) of the NLC dispersion in a 0.45-μm PVDF membrane (Millipore, Billerica, USA). The BZN concentration solubilized in the external aqueous phase was determined after 0.45 μm filtration and ultrafiltration (Amicon 100 k, Millipore, Billerica, USA) and was negligible.

Thus, 200 μL of the nanoparticle dispersion in both conditions (total and filtered) was dissolved in tetrahydrofuran (4 mL) and diluted to 5 mL in methanol to be analyzed by HPLC. The EE was then calculated using the equation:

$$EE\ (\%) = \frac{\text{filtered [BZN]}}{\text{total [BZN]}} \times 100$$

Stability of the nanoparticle dispersion

The NLC-BZN formulations (n = 3) were stored at 4 °C, protected from light, and monitored as the average diameter, PDI, ZP, and pH at 0, 7, 14, and 28 days. BZN retention was also monitored considering the percentage of BZN kept encapsulated in the nanocarrier throughout the time (vs. time 0).

Freeze-drying conditions

The NLC-BZN and b-NLC water dispersion were frozen in liquid nitrogen for 5 min and lyophilized in a Labconco FreeZone 4.5-L freeze-dryer (Kansas, EUA) for 24 h at -50 ºC for further characterization.

Characterization of lyophilized NLC-BZN (L-NLC-BZN)

Fourier transform infrared spectroscopy (FTIR)

FTIR absorption spectra were obtained from a Varian 640-IR spectrophotometer (Palo Alto, USA) equipped with attenuated total reflectance mode. Spectra were obtained for the formulation components in the physical state, the lyophilized b-NLC and NLC-BZN, and the physical mixture (b-NLC + BZN) at room temperature using a diamond crystal with 4 cm^{-1} resolution and 32 accumulations.

Powder X-ray diffraction

PXRD data were collected in an XRD-7000 diffractometer (Shimadzu, Kyoto, Japan) at room temperature under 40 kV and 30 mA using CuKα (λ = 1.54056Å) equipped with polycapillary focusing optics under parallel geometry coupled with a graphite monochromator. The sample was spun at 60 rpm and scanned over an angular range of 2–40° (2θ) with a step size of 0.02° (2θ) and a time constant of 2s/step. All fitting procedures were obtained using FullProf Suite.

For the thin film experiment, conditions were room temperature under 40 kV and 35 mA using CuKα (λ = 1.54056Å) equipped with polycapillary focusing optics under parallel geometry coupled with a graphite monochromator, rising angle of 1°, in a static sample setup, and using 0.02° (2θ) as step increment and time constant of 4s/step.

Thermal analysis

Differential scanning calorimetry (DSC) and thermogravimetry (TG) analyses were performed for the solid formulation components (BZN, Compritol, and poloxamer 407), and the lyophilized formulations L-b-NLC and L-NLC-BZN. The DSC curves were obtained in a DSC60 Shimadzu cell (Tokyo, Japan) and calibrated with indium (T_{onset} = 156.63 °C, ΔH_{fus} = 28.45 J/g) under the following conditions: dynamic nitrogen atmosphere at 50 mL/min, a heating rate of 10 °C/min, from 30 to 400 °C, and sample mass of about 1.5 mg accurately weighed in a closed alumina crucible. The TG curves were obtained using a Shimadzu DTG60 thermobalance (Tokyo, Japan) with a heating rate of 10 °C/min, from 30 to 600 °C, dynamic nitrogen atmosphere of 50 mL/min, and sample mass of about 2.5 mg accurately weighed in an aluminum crucible.

In vitro membrane toxicity studies

In vitro membrane toxicity studies were performed according to Scalise *et al.* (2016), with few modifications. In summary, 100 µL of the 4% RBC suspension and 100 µL of the treatments (BZN solution, b-NLC, and NLC-BZN) were added to a 96-well plate in BZN concentrations of 12.5, 25, 50, and 100 µg/mL. The negative control was a saline solution (0.9% w/v), and the positive control was a 1% (w/v) saponin solution. The plates were then shaken for 1 h (400 rpm; 37 °C) and centrifuged (3000 rpm; 15 min). The supernatant was collected, and the amount of released hemoglobin was determined by UV spectrophotometry at 540 nm. The percentage release of hemoglobin was calculated using the equation:

$$\text{Released hemoglobin (\%)} = \frac{\text{Abs}_{\text{sample}}}{\text{Abs}_{\text{positive control}}} \times 100$$

Flávia L. O. Silva, Maria B. F. Marques, Maria I. Yoshida, Wagner N. Mussel, João V. W. Silveira, Poliana R. Barroso, Kelly C. Kato, Helen R. Martins, Guilherme Carneiro

Cell viability studies

In vitro cytotoxicity studies were conducted in L929 cells (mouse fibroblasts) grown in RPMI 1640 medium supplemented with 10% FBS, 3.2 mM L-glutamine, 100 µg/mL streptomycin, and 100 IU/mL penicillin in a humidified incubator with 5% CO_2 at 37 °C. The L929 cells (1.0×10^4 cells/well) were seeded in 96-well plates and incubated for 24 h. After this time, the treatments (free BZN solution and NLC-BZN) were added to the plates in the range of 1.95 to 125 µg/mL, and a 0.02 M cadmium chloride solution was utilized as a positive control. After 72 h of incubation, 20 µL of an MTT solution (3 mg/mL) was added to each well, and the microplates were incubated at 37 °C for 4 h. Afterward, the supernatant was discarded, and DMSO was added to dissolve the formazan crystals. The metabolic activity was estimated as the MTT conversion rate by measuring the absorbance at 540 nm (Mosmann, 1983). The absorbance of wells with non-treated cells was considered 100% cell viability, and the results from three independent experiments were expressed as the relative percentage of cell viability, and CC_{50} was determined.

Trypanocidal activity

The trypanocidal activity of NLC-BZN was investigated using epimastigotes of the Colombian strain of *T. cruzi*, which is considered a prototype of resistance to BZN (Filardi, Brener, 1987). The strain was harvested in LIT medium supplemented with 10% FBS, 0.2% streptomycin solution (100 µg/mL), and 0.18% hemin solution (10 mg/mL). The culture was maintained in a biochemical oxygen demand (BOD) incubator at 26 ºC, and the experiments were performed after the strain reached the stationary phase.

The *T. cruzi* strain (2.0×10^6 parasite/well) was seeded into 96-well plates, and the treatments were added: free BZN solution and NLC-BZN, in the range of 1.95 to 250 µg/mL; b-NLC was diluted in the same way as NLC-BZN. The plates were incubated at 26 ºC in the BOD incubator for 72 h, then the viable parasites in the supernatant were counted in a Neubauer chamber (Bortoluzzi *et al.*, 2021; Pereira *et al.*, 2021). The number of parasites from the untreated wells was considered as 100% cell viability. Results from three independent experiments were expressed as the relative percentage of cell viability, and the 50% inhibitory concentration (IC_{50}) was also determined for the treatments.

Statistical analysis

The results were represented as mean value ± standard deviation from determinations in triplicate. One-way analysis of variance (ANOVA) followed by Tukey's test was used to analyze the statistical differences among the mean values (α = 0.05). Data from cell viability were analyzed by two-way ANOVA followed by Bonferroni post-test (α = 0.05).

RESULTS AND DISCUSSION

Formulation development

Despite the undeniable importance of BZN as an antichagasic drug, its properties are not favorable for oral administration: low aqueous solubility (0.4 mg/mL) and irregular absorption, resulting in unfavorable pharmacokinetics (Maximiano *et al.*, 2011a). Incorporating these poorly water-soluble drugs into lipid nanoparticles can be an alternative for increasing drug bioavailability and stability in physiological conditions, including those found in the gastrointestinal tract, while comprising a stable and versatile product. Other lipid nanocarriers, such as liposomes and nanoemulsions, may be unstable in the gastrointestinal tract or during storage (Gaba *et al.*, 2015; Beloqui *et al.*, 2017).

Four parameters were varied in the optimization stage of the BZN-loaded NLC: the liquid lipids, the composition of the surfactant system, the total lipid/surfactant ratio, and the amount of BZN initially added for encapsulation, according to the composition described in Table I. All formulations were screened and optimized to find the smallest size with homogenous distribution, higher ZP (in absolute values), and higher EE. Thus, the changes performed in the composition

of liquid lipids and inclusion of Chol had negligible influence on the particle size and PDI, which remained near 115 nm and 0.25, respectively (p > 0.05). However, EE drastically reduced from 83.0% (NLC A) to 74.5% (NLC B) and 74.2% (NLC C), which was likely a result of the different BZN solubility in the lipid combinations (Table I). Thus, the MCT was chosen as the liquid lipid in the lipid matrix.

Nonetheless, in these initial formulations containing only TW80 as a surfactant, BZN was released only a few hours after the NLC preparation, clearly indicating poor encapsulation stability (50–60% release after 3–4 h). The surfactant system was then varied in mixtures of TW80 with P407, SL or EL, and P407 alone. NLC F (containing TW80 + P407) was the most promising, as it had a similar diameter, ZP, and EE of the initial NLC A (only TW80), albeit PDI decreased to 0.19 (Table I), indicating a more homogeneous size distribution and lack of initial release of BZN. Larger particle sizes and lower EE were observed in the other formulations: NLCs D, E, and G (when only P407 was utilized). The ZP was negative in all formulations, ranging from -15.9 to -46.0 mV, which may be associated with the presence of ionized free fatty acids at the interface of the particle, naturally present in the lipids and surfactants: MCT, soybean oil, lecithin, and Compritol (Bruxel *et al.*, 2012).

To increase the BZN encapsulation, some changes in the total lipid/surfactant ratio were proposed. However, only increased particle size (up to 330 nm) was found in NLC H and I without increasing the EE (Table I). In fact, increased diameter is expected with a higher total lipid/surfactant ratio, although the use of higher quantities of lipids is better justified with higher encapsulation, as the excessive increase in the lipid content is associated with higher cytotoxicity caused by the increase of free fatty acids resulting from the enzymatic degradation of the lipid matrix (Scholer *et al.*, 2002; Ridolfi *et al.*, 2011).

Therefore, the lipid matrix of NLC F was utilized in the final analyses.

Finally, the BZN concentration was increased to 0.1 and 0.2% (w/w), although the EE decreased from 82.6 to 38.3 and 18.9%, respectively. The nominal concentration of BZN encapsulated practically remained the same (0.38–0.41 mg/mL), indicating possible saturation of the nanocarrier. Moreover, drug loading (encapsulated drug/total lipid matrix content ratio) was 1.64%, which is higher than that obtained for other previously developed BZN lipid systems (Morilla *et al.*, 2004; Morilla, Prieto, Romero, 2005; Streck *et al.*, 2014; Streck *et al.*, 2016; Vinuesa *et al.*, 2017).

Therefore, NLC F (with 0.05% BZN) was considered the optimized formulation. This product had 100% of the particles with an average diameter below 500 nm and 85.9% below 200 nm, meeting the particle size requirements for oral and even intravenous administration (USP39-NF34, 2016). The low mean diameter of this optimized NLC-BZN (110 nm), with a narrow size distribution (PI = 0.19), is also associated with higher cellular uptake and high absorption when compared with larger nanoparticles (Li *et al.*, 2016; Beloqui *et al.*, 2017; Danaei *et al.*, 2018).

All analyzed parameters (diameter, PI, ZP, and pH) of the optimized NLC-BZN remained stable for up to 28 days (Figure 1). There was no change (p > 0.05) in the concentration of BZN retained in the matrix, and only a reduction of roughly 6.2% was detected after 28 days. The increase in the nanoparticle size usually precedes other macroscopic changes and is a good indicator of instability (Bahari, Hamishehkar, 2016). The negative ZP, together with the presence of ethoxylated surfactants (TW80 and P407), hinder the natural tendency of nanoparticle aggregation either by electrostatic repulsion or steric hindrance of the hydrophilic polyethylene oxide chains coating the nanoparticle surface (Wulff-Perez *et al.*, 2012; Beloqui *et al.*, 2017).

Flávia L. O. Silva, Maria B. F. Marques, Maria I. Yoshida, Wagner N. Mussel, João V. W. Silveira,
Poliana R. Barroso, Kelly C. Kato, Helen R. Martins, Guilherme Carneiro
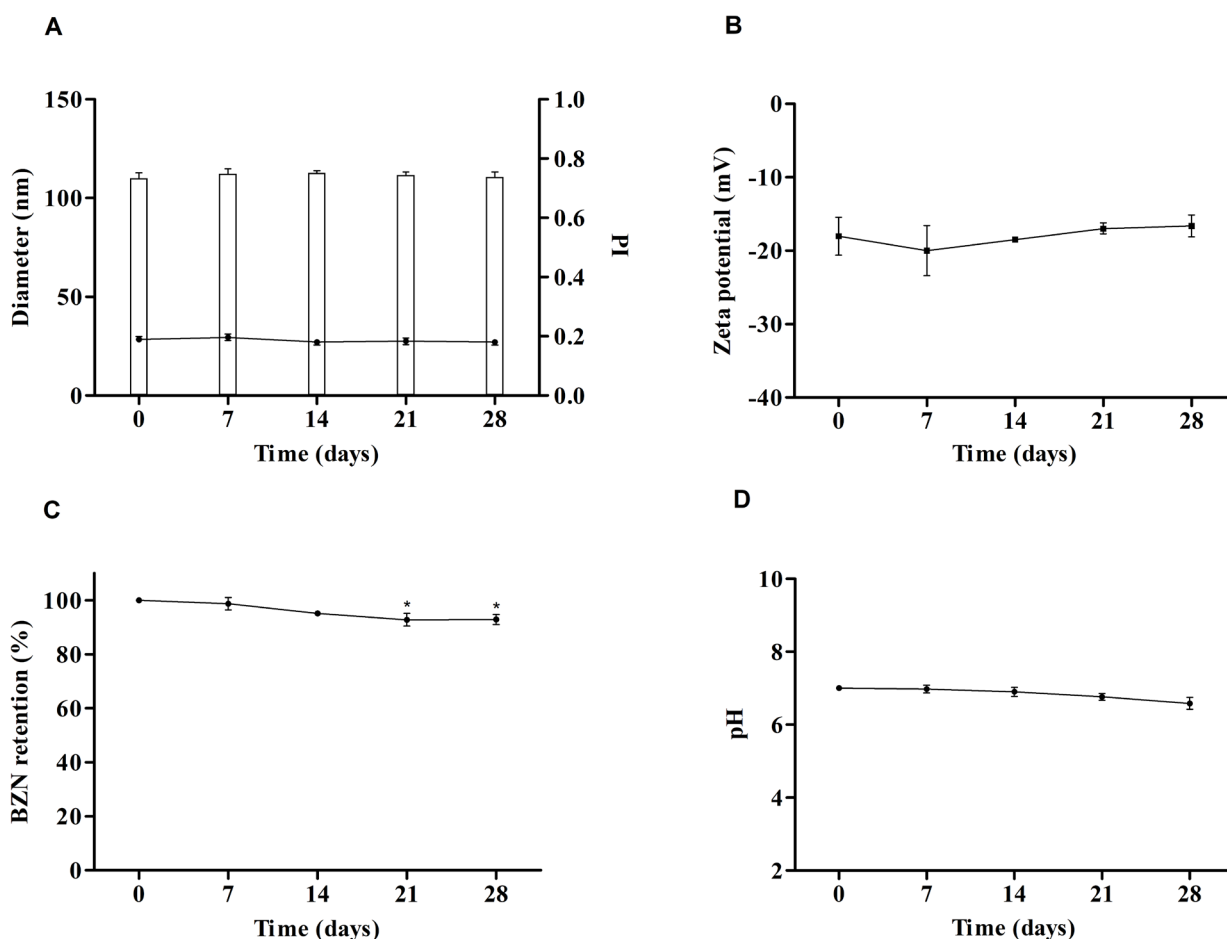
FIGURE 1 - Stability of NLC-BZN over 28 days, particle size and PI (a), ZP (b), BZN retention (c), and pH (D).

Fourier transform infrared spectroscopy

The FTIR absorption spectra for the pure materials of the NLC-BZN are shown in Figure 2A. All characteristic absorption bands were observed for the pure components, with the corresponding wavenumber (cm^{-1}) and intensity summarized in Table II. The FTIR spectrum of b-NLC (Figure 2B) showed a full and robust band at 3400–3200 cm^{-1} (O–H from glycerol) and in the range of 2900–2700 cm^{-1} (C–H stretch from the various components). The absorption spectra of NLC-BZN and b-NLC had a similar profile, and the characteristic bands of BZN (3330, 1685, 1660–1500, and 1250–1000 cm^{-1}) could only be observed in the spectrum of the physical mixture. Together with the high EE values, this may indicate BZN encapsulation inside the lipid matrix.
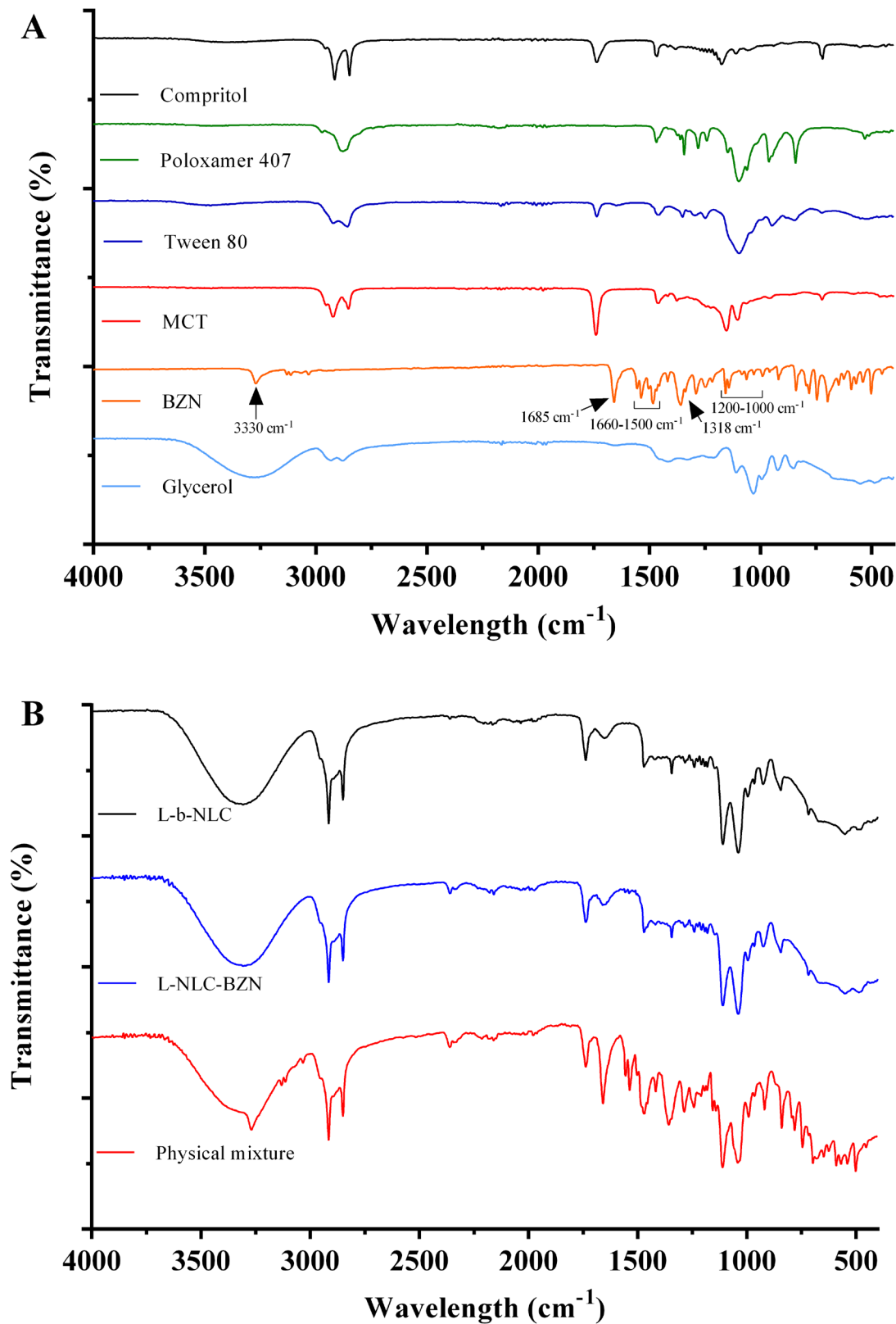
FIGURE 2 - FTIR spectra of BZN and the pure formulation components (a); lyophilized formulation (blank and loaded with BZN), and the physical mixture (b). BZN main peaks were highlighted in the respective spectrum.

Flávia L. O. Silva, Maria B. F. Marques, Maria I. Yoshida, Wagner N. Mussel, João V. W. Silveira, Poliana R. Barroso, Kelly C. Kato, Helen R. Martins, Guilherme Carneiro

TABLE II - Main IR absorption bands of the isolated formulation components, with their attributions and classification by intensity

Wavenumber (cm⁻¹)	Attributions	Intensity	Reference
Compritol			
2849	C–H (stretch)	Medium	(Rahman, Zidan, Khan, 2010; Abu-rahma, Badr-Eldin, 2014)
2815	C–H (stretch)	Medium	
1740	C=O (stretch)	Medium	
1500-700	-(CH$_2$)$_n$- (numerous vibrational bands)	Medium	
Poloxamer 407			
2893	Aliphatic C–H (stretch)	Medium	(Garala et al., 2013)
1355	O–H (in plane bend)	Medium	
1125	C–O (stretch)	Medium	
Tween 80			
2930	–CH$_2$ (stretch)	Medium	(Li et al., 2012)
2860	–CH$_2$ (stretch)	Medium	
1735	C=O (stretch of esters)	Medium	
1458	–CH$_3$ (symmetrical and asymmetric bend)	Medium	
1351	–CH$_3$ (symmetrical and asymmetric bend)	Medium	
1100	C–O–C (stretch of esters)	Weak	
MCT			
2956	C–H (stretch)	Medium	(Kiefer et al., 2016)
2923	C–H (stretch)	Medium	
2854	C–H (stretch)	Medium	
1744	C=O (stretch)	Medium	
BZN			
3330	N–H (stretch)	Strong	(Soares-Sobrinho et al., 2010; de Melo et al., 2017)
1685	C=O (stretch of amides)	Strong	
1660-1500	N–O (stretch in NO$_2$ groups)	Strong	
1500-1420	C–C (aromatic ring stretch)	Strong	
1318	C–N (stretch)	Strong	
1200-1000	C–H (aromatic axial deformation)	Medium	
Glycerol			
3400-3200	O–H (stretch)	Medium	(Glavcheva-Laleva et al., 2015)
2960-2850	C–H (stretch)	Medium	

Powder X-ray diffraction

As shown in the diffractograms in Figure 3A, Compritol showed two diffraction peaks for NLC-BZN, a high-intensity peak at 21.2º 2θ and a lower intensity peak at 23.4º 2θ, with the characteristic values for the β' form of the lipids (Fini *et al.*, 2011). Poloxamer 407 showed two characteristic high-intensity peaks at 19.4º and 23.5º 2θ, as described elsewhere (Garcia-Millan, Quintans-Carballo, Otero-Espinar, 2017). Furthermore, BZN presented a typical crystalline diffraction pattern, exhibiting sharp peaks at 11.0º, 16.9º, 21.9º, and 25.2º 2θ, a similar profile observed in previous reports (Palmeiro-Roldan *et al.*, 2014).

In the experiment with the thin film (Figure 3A, solid thin line), NLC-BZN did not show the characteristic signal of BZN at about 20.5° 2θ, indicating that BZN is not present at the surface of the sample. Thus, during the nanoparticle preparation and in contact with the lipids of the matrix, BZN may have undergone drug amorphization or molecular solubilization, which could have contributed to encapsulating BZN in the lipid matrix, thereby corroborating the high EE values.

Thermal analysis

The DSC curve of BZN showed an endothermic event at 188.38 °C ($\Delta H = 133.01$ J/g), corresponding to the melting point (Soares-Sobrinho *et al.*, 2010). An exothermic event starting at 220 °C, characteristic of drug decomposition (Figure 3B), was confirmed by the loss of mass in the same temperature on the TG curve (Figure 3C). The endothermic events of Compritol ($T_{onset} = 69.60$ °C; $\Delta H = 117.76$ J/g) and Poloxamer 407 ($T_{onset} = 51.39$ °C; $\Delta H = 117.48$ J/g) were also consistent with the melting point described (Fini *et al.*, 2011).

The thermal behavior for both NLC-BZN and b-NLC formulations were similar, with a single endothermic event at 64.07 and 63.74 ºC ($\Delta H = 85.79$ and 87.40 J/g), respectively (Figure 3B), without loss of mass in the TG curve, which was associated with the melting of the nanocarriers. The formulations presented thermal stability up to 238 ºC, a higher temperature than BZN alone. At this temperature, the decomposition process begins, with a 93% loss of mass in two stages (Figure 3C).

Therefore, the high EE obtained for BZN in the optimized NLC formulation was also observed in the FTIR, PXRD, DSC, and TG studies due to the similarities observed between the signals of the BZN-loaded NLC and the blank formulation (without BZN, b-NLC). As observed in the other characterization studies, the missing signals of BZN in the NLC-BZN analyses are also indicators of this high encapsulation. The broad and partially symmetrical edges of the peaks found in the DSC curve of the b-NLC and NLC-BZN are typical of complex systems, such as multicomponent carriers. The observed decrease in the melting enthalpy of NLC compared to the pure Compritol is evidence of the lower crystallinity degree of the NLC matrix (Li *et al.*, 2009; Gonullu *et al.*, 2015; Argimón *et al.*, 2016). Since none of the thermal events attributed to the NLC-BZN were exclusively assigned to any of the isolated raw materials, one can assume that a singular formulation with specific physicochemical characteristics was produced, and the selected proportion of each component was solely part of the nanoparticle composition (Bunjes, Unruh, 2007).
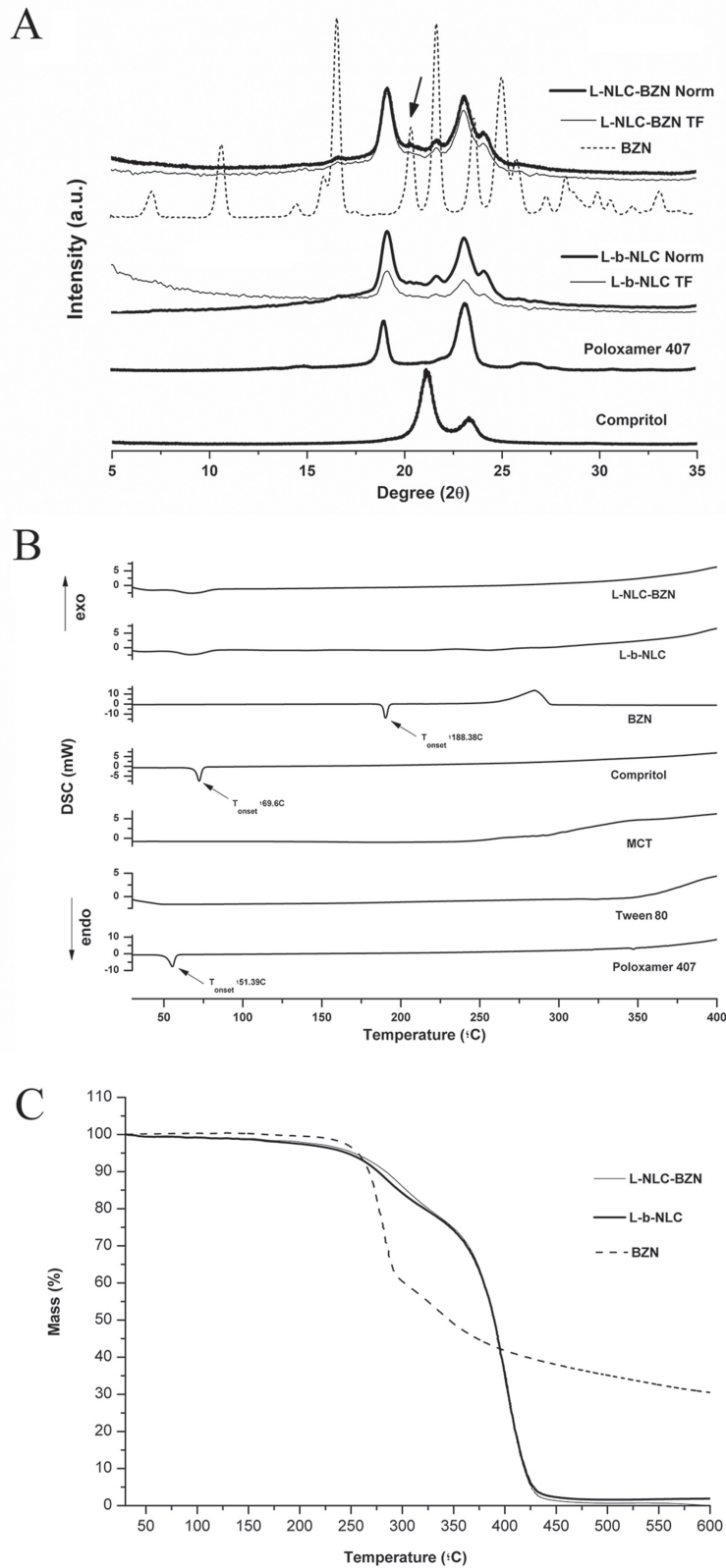
FIGURE 3 - Diffractograms of the pure components and lyophilized formulations (blank and loaded with BZN) in the thin film (TF) and normal (Norm) experiments (a). DSC curves of the pure components and lyophilized formulations obtained in nitrogen atmosphere (b). TG curves of the pure components and lyophilized formulations obtained in nitrogen atmosphere (c).

Membrane toxicity studies

The next step was investigating the *in vitro* toxicity of the developed BZN nanocarriers. The RBCs are an indicative model of membrane toxicity and a straightforward method since the hemolytic activity promotes hemoglobin release from RBC, which can be quantified by spectrophotometry (de Freitas *et al.*, 2008). Percentage hemoglobin release was low (<9%), even at the highest concentration (100 µg/mL), regardless of the treatments applied (Figure 4A). Similar findings were previously obtained by Scalise *et al.* (2016) for BZN nanocrystals (6% hemolysis at 100 µg/mL) and conventional BZN (9% hemolysis at 50 µg/mL).

Moreover, the percentage of hemoglobin release was even lower (<3%) for nanocarrier treatment (b-NLC and NLC-BZN). At the highest concentration tested (100 µg/mL), there were no significant differences between the hemolysis caused by free or encapsulated BZN, indicating the low toxicity of NLC-BZN to membranes by direct contact.

Cell viability

The L929 cell viability (human fibroblasts) was dose-dependent after 72 h of treatment (Figure 4B), and NLC-BZN was less cytotoxic for L929 cells than free BZN. For instance, the cytotoxicity of free BZN (16.8 ± 2.0%) was higher than NLC-BZN (56.5 ± 7.1%) at the concentration of 125 µg/mL, and a similar profile was observed at the other concentrations. The CC_{50} determined for NLC-BZN (110.7 ± 1.1 µg/mL) was twice the value of free BZN (51.3 ± 1.1 µg/mL for BZN).

After 72 h, the treatment with free BZN was clearly more cytotoxic for L929 cells than the NLC-BZN, indicating favorable biocompatibility of the developed lipid nanoparticles. The toxicity of BZN in mammalian cells seems to be associated with non-specific and highly reactive electrophilic metabolites (Castro, de Mecca, Bartel, 2006), and its encapsulation should reduce cytotoxicity in normal cells. Nonetheless, a previous study developed a BZN-loaded microemulsion and reported drastically reduced Vero cell viability (10% at 80 µg/mL) after only 12 h of contact time, clearly showing more intense cytotoxicity than the formulation developed herein (Streck *et al.*, 2016).

Trypanocidal activity

At the highest concentration (125 µg/mL), BZN and NLC-BZN induced a 100% reduction in the viability of the BZN-resistant Colombian strain of *T. cruzi* (Soeiro *et al.*, 2013). No significant effect was observed in the treatment with the blank NLC (without BZN), and the viability of the epimastigotes was similar to the cell viability control (Figure 4C). Both free BZN and NLC-BZN showed a dose-dependent relationship with cell viability, although the effect of BZN encapsulation was more remarkable in concentrations above 3.90 µg/mL (p < 0.05). These data suggest that encapsulation in nanoparticles increased BZN activity in this *T. cruzi* strain. The IC_{50} for the free BZN against this strain (26.7 ± 0.1 µM) was comparable to the previous reports: 14.9–26.8 µM (Vinuesa *et al.*, 2017), 25.4 ± 2.7 µM (Moreno *et al.*, 2010), 34.1 ± 0.8 µM (Zingales *et al.*, 2015), and 4.1 ± 1.1 µg/mL (Meira *et al.*, 2015). The IC_{50} was lower for NLC-BZN (20.2 ± 0.4 µM), which is considered more effective than free BZN against this BZN-resistant strain, thus highly promising for further *in vivo* research.

Flávia L. O. Silva, Maria B. F. Marques, Maria I. Yoshida, Wagner N. Mussel, João V. W. Silveira, Poliana R. Barroso, Kelly C. Kato, Helen R. Martins, Guilherme Carneiro
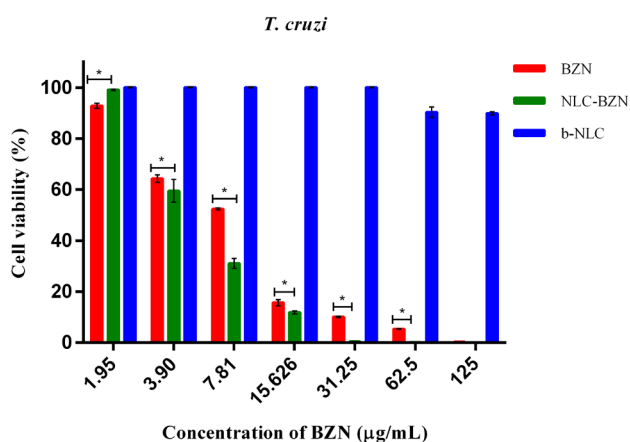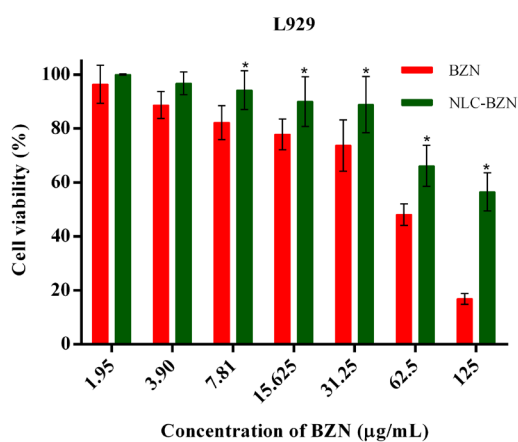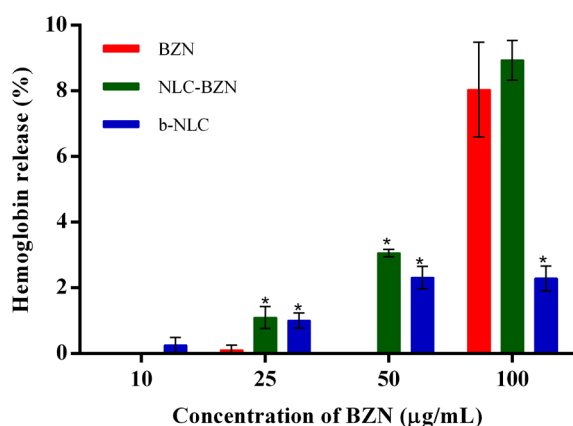
FIGURE 4 - Percentage of hemoglobin release after contact of RBC with BZN, NLC-BZN, and b-NLC (a). Viability of L929 cells after 72 h of treatment with BZN and NLC-BZN (b). Cell viability of *T. cruzi* epimastigotes after 72 h of treatment with BZN, NLC-BZN, and b-NLC (c).

Lipid nanoparticles (NLC) loaded with BZN were screened and developed with favorable physicochemical characteristics for oral and parenteral administration.

High EE and drug loading were obtained, superior to previously reported lipid systems. The FTIR, thermal, and crystallinity studies indicated nanoparticle formation with high drug encapsulation. Compared to the free BZN, the developed BZN-loaded NLC showed lower toxicity for membranes and fibroblast cells, which was associated with increased trypanocidal efficacy against the BZN-resistant Colombian strain of *T. cruzi*. Therefore, this novel formulation has promising potential in Chagas disease treatment and must be further studied in more complex models, such as *in vivo* experiments.

STATEMENTS AND DECLARATIONS

ACKNOWLEDGEMENTS

CONFLICTS OF INTEREST:

The authors have no conflicts of interest to declare that are relevant to the content of this article.

FUNDING:

REFERENCES

Aburahma MH, Badr-Eldin SM. Compritol 888 ATO: a multifunctional lipid excipient in drug delivery systems and nanopharmaceuticals. Expert Opin Drug Deliv. 2014,11(12):1865-1883.

Almeida OP, Marcial SPS, Gouveia FPP, Carneiro G. Validation of a chromatographic analytical method for quantification of benznidazole incorporated in nanostructured lipid formulations. J Braz Chem Soc. 2016;28(2):236-241.

Argimón M, Romero M, Miranda P, Mombrú Á, Miraballes I, Zimet P, et al. Development and characterization of vitamin

A-Loaded solid lipid nanoparticles for topical application. J Braz Chem Soc. 2016;28(07):1177-1184.

Bahari LAS, Hamishehkar H. The impact of variables on particle size of solid lipid nanoparticles and nanostructured lipid carriers; a comparative literature review. Adv Pharm Bull. 2016;6(2):143-151.

Beloqui A, del Pozo-Rodríguez A, Isla A, Rodríguez-Gascón A, Solinís MÁ. Nanostructured lipid carriers as oral delivery systems for poorly soluble drugs. J Drug Deliv Sci Technol. 2017;42:144-154.

Bortoluzzi AAM, Staffen IV, Banhuk FW, Griebler A, Matos PK, Ayala TS, et al. Determination of chemical structure and anti-Trypanosoma cruzi activity of extracts from the roots of Lonchocarpus cultratus (Vell.) A.M.G. Azevedo & H.C. Lima. Saudi J Biol Sci. 2021;28(1):99-108.

Branquinho RT, Mosqueira VC, de Oliveira-Silva JC, Simoes-Silva MR, Saude-Guimaraes DA, de Lana M. Sesquiterpene lactone in nanostructured parenteral dosage form is efficacious in experimental Chagas disease. Antimicrob Agents Chemother. 2014;58(4):2067-2075.

Bruxel F, Laux M, Wild LB, Fraga M, Koester LS, Teixeira HF. Nanoemulsões como sistemas de liberação parenteral de fármacos. Quim Nova. 2012;35(9):1827-1840.

Bunjes H, Unruh T. Characterization of lipid nanoparticles by differential scanning calorimetry, X-ray and neutron scattering. Adv Drug Deliv Rev. 2007;59(6):379-402.

Castro JA, de Mecca MM, Bartel LC. Toxic side effects of drugs used to treat Chagas' disease (American trypanosomiasis). Hum Exp Toxicol. 2006;25(8):471-479.

Danaei M, Dehghankhold M, Ataei S, Hasanzadeh Davarani F, Javanmard R, Dokhani A, et al. Impact of particle size and polydispersity index on the clinical applications of lipidic nanocarrier systems. Pharmaceutics. 2018;10(2):57.

de Freitas MV, Netto Rde C, da Costa Huss JC, de Souza TM, Costa JO, Firmino CB, et al. Influence of aqueous crude extracts of medicinal plants on the osmotic stability of human erythrocytes. Toxicol In Vitro. 2008;22(1):219-224.

de Melo PN, de Caland LB, Fernandes-Pedrosa MF, da Silva-Júnior AA. Designing and monitoring microstructural properties of oligosaccharide/co-solvent ternary complex particles to improve benznidazole dissolution. J Mater Sci. 2017,53(4):2472-2483.

Fernandes RS, Silva JO, Seabra HA, Oliveira MS, Carregal VM, Vilela JMC, et al. alpha- Tocopherol succinate loaded nano-structed lipid carriers improves antitumor activity of doxorubicin in breast cancer models in vivo. Biomed Pharmacother. 2018;103:1348-1354.

Ferraz LRM, Alves AEG, Nascimento D, Amariz IAE, Ferreira AS, Costa SPM, et al. Technological innovation strategies for the specific treatment of Chagas disease based on Benznidazole. Acta Trop. 2018;185:127-132.

Filardi LS, Brener Z. Susceptibility and natural resistance of Trypanosoma cruzi strains to drugs used clinically in Chagas disease. Trans R Soc Trop Med Hyg. 1987;81(5):755-759.

Fini A, Cavallari C, Ospitali F, Gonzalez-Rodriguez ML. Theophylline-loaded compritol microspheres prepared by ultrasound-assisted atomization. J Pharm Sci. 2011;100(2):743-757.

Fonseca-Berzal C, Palmeiro-Roldan R, Escario JA, Torrado S, Aran VJ, Torrado-Santiago S, et al. Novel solid dispersions of benznidazole: preparation, dissolution profile and biological evaluation as alternative antichagasic drug delivery system. Exp Parasitol. 2015;149:84-91.

Gaba B, Fazil M, Ali A, Baboota S, Sahni JK, Ali J. Nanostructured lipid (NLCs) carriers as a bioavailability enhancement tool for oral administration. Drug Deliv. 2015;22(6):691-700.

Garala K, Joshi P, Shah M, Ramkishan A, Patel J. Formulation and evaluation of periodontal in situ gel. Int J Pharm Investig. 2013,3(1):29-41.

Garcia-Millan E, Quintans-Carballo M, Otero-Espinar FJ. Solid-state characterization of triamcinolone acetonide nanosuspensiones by X-ray spectroscopy, ATR Fourier transforms infrared spectroscopy and differential scanning calorimetry analysis. Data Brief. 2017;15:133-137.

Glavcheva-Laleva Z, Kerekov S, Pavlov D, Glavchev I. Obtaining of modifiers for reduced friction by esterification of waste glycerol from biodiesel production and sylfat 2. Chem Eng Sci. 2015;3(1):1-6.

Gonullu U, Uner M, Yener G, Karaman EF, Aydogmus Z. Formulation and characterization of solid lipid nanoparticles, nanostructured lipid carriers and nanoemulsion of lornoxicam for transdermal delivery. Acta Pharm. 2015;65(1):1-13.

Kiefer J, Frank K, Zehentbauer FM, Schuchmann HP. Infrared spectroscopy of bilberry extract water-in-oil emulsions: sensing the water-oil interface. Biosensors (Basel). 2016,6(2):13.

Lamas MC, Villaggi L, Nocito I, Bassani G, Leonardi D, Pascutti F, et al. Development of parenteral formulations and evaluation of the biological activity of the trypanocide drug benznidazole. Int J Pharm. 2006;307(2):239-243.

Leonardi D, Salomon CJ. Unexpected performance of physical mixtures over solid dispersions on the dissolution behavior of benznidazole from tablets. J Pharm Sci. 2013;102(3):1016-1023.

Leonardi D, Salomon CJ, Lamas MC, Olivieri AC. Development of novel formulations for Chagas' disease: optimization of benznidazole chitosan microparticles based on artificial neural networks. Int J Pharm. 2009;367(1-2):140-147.

Li H, Chen M, Su Z, Sun M, Ping Q. Size-exclusive effect of nanostructured lipid carriers on oral drug delivery. Int J Pharm. 2016;511(1):524-537.

Li HJ, Zhang AQ, Hu Y, Sui L, Qian DJ, Chen M. Large-scale synthesis and self-organization of silver nanoparticles with Tween 80 as a reductant and stabilizer. Nanoscale Res Lett. 2012,7(1):612.

Li Z, Yu L, Zheng L, Geng F. Studies on crystallinity state of puerarin loaded solid lipid nanoparticles prepared by double emulsion method. J Therm Anal Calorim. 2009;99(2):689-693.

Lima AA, Soares-Sobrinho JL, Silva JL, Correa-Junior RA, Lyra MA, Santos FL, et al. The use of solid dispersion systems in hydrophilic carriers to increase benzonidazole solubility. J Pharm Sci. 2011;100(6):2443-2451.

Marcial SPdS, Carneiro G, Leite EA. Lipid-based nanoparticles as drug delivery system for paclitaxel in breast cancer treatment. J Nanopart Res. 2017;19(10):340.

Maximiano FP, Costa GH, de Sa Barreto LC, Bahia MT, Cunha-Filho MS. Development of effervescent tablets containing benzonidazole complexed with cyclodextrin. J Pharm Pharmacol. 2011a;63(6):786-793.

Maximiano FP, Costa GHY, Souza Jd, Cunha-Filho MSSd. Caracterização físico-química do fármaco antichagásico benznidazol. Quim Nova. 2010;33(8):1714-1719.

Maximiano FP, de Paula LM, Figueiredo VP, de Andrade IM, Talvani A, Sa-Barreto LC, et al. Benznidazole microcrystal preparation by solvent change precipitation and in vivo evaluation in the treatment of Chagas disease. Eur J Pharm Biopharm. 2011b;78(3):377-384.

Meira CS, Guimaraes ET, Dos Santos JA, Moreira DR, Nogueira RC, Tomassini TC, et al. In vitro and in vivo antiparasitic activity of Physalis angulata L. concentrated ethanolic extract against Trypanosoma cruzi. Phytomedicine. 2015;22(11):969-974.

Moreno M, D'Avila DA, Silva MN, Galvao LM, Macedo AM, Chiari E, et al. Trypanosoma cruzi benznidazole susceptibility in vitro does not predict the therapeutic outcome of human Chagas disease. Mem Inst Oswaldo Cruz. 2010;105(7):918-924.

Morilla MJ, Benavidez P, Lopez MO, Bakas L, Romero EL. Development and in vitro characterisation of a benznidazole liposomal formulation. Int J Pharm. 2002;249(1-2):89-99.

Morilla MJ, Montanari JA, Prieto MJ, Lopez MO, Petray PB, Romero EL. Intravenous liposomal benznidazole as trypanocidal agent: increasing drug delivery to liver is not enough. Int J Pharm. 2004;278(2):311-318.

Morilla MJ, Prieto MJ, Romero EL. Benznidazole vs benznidazole in multilamellar liposomes: how different they interact with blood components? Mem Inst Oswaldo Cruz. 2005;100(2):213-219.

Morilla MJ, Romero EL. Nanomedicines against Chagas disease: an update on therapeutics, prophylaxis and diagnosis. Nanomedicine (Lond). 2015;10(3):465-481.

Mosmann T. Rapid colorimetric assay for cellular growth and survival: application to proliferation and cytotoxicity assays. J Immunol Methods. 1983;65(1–2):55–63.

Pan American Health Organization (PAHO). Enfermedade de Chagas. 2020. Available at https://www.paho.org/hq/index.php?option=com_topics&view=article&id=10&Itemid=40743&lang=es.

Palmeiro-Roldan R, Fonseca-Berzal C, Gomez-Barrio A, Aran VJ, Escario JA, Torrado-Duran S, et al. Development of novel benznidazole formulations: physicochemical characterization and in vivo evaluation on parasitemia reduction in Chagas disease. Int J Pharm. 2014;472(1-2):110-117.

Pereira PML, Camargo PG, Fernandes BT, Flores-Junior LAP, Dias LRS, Lima CHS, et al. In vitro evaluation of antitrypanosomal activity and molecular docking of benzoylthioureas. Parasitol Int. 2021;80:102225.

Perez-Molina JA, Molina I. Chagas disease. Lancet. 2018;391(10115):82-94.

Prata A. Clinical and epidemiological aspects of Chagas disease. Lancet Infect Dis. 2001;1(2):92-100.

Rahman Z, Zidan AS, Khan MA. Non-destructive methods of characterization of risperidone solid lipid nanoparticles. Eur J Pharm Biopharm. 2010,76(1):127-137.

Ridolfi DM, Marcato PD, Machado D, Silva RA, Justo GZ, Durán N. In vitro cytotoxicity assays of solid lipid nanoparticles in epithelial and dermal cells. J Phys: Conf Ser. 2011;304:012032.

Romero EL, Morilla MJ. Nanotechnological approaches against Chagas disease. Adv Drug Deliv Rev. 2010;62(4-5):576-588.

Salomon CJ. First century of Chagas' disease: an overview on novel approaches to nifurtimox and benzonidazole delivery systems. J Pharm Sci. 2012;101(3):888-894.

Scalise ML, Arrua EC, Rial MS, Esteva MI, Salomon CJ, Fichera LE. Promising efficacy of benznidazole nanoparticles

in acute Trypanosoma cruzi murine model: In-Vitro and In-Vivo studies. Am J Trop Med Hyg. 2016;95(2):388-393.

Scholer N, Hahn H, Muller RH, Liesenfeld O. Effect of lipid matrix and size of solid lipid nanoparticles (SLN) on the viability and cytokine production of macrophages. Int J Pharm. 2002;231(2):167-176.

Seremeta KP, Arrua EC, Okulik NB, Salomon CJ. Development and characterization of benznidazole nano- and microparticles: A new tool for pediatric treatment of Chagas disease? Colloids Surf B. 2019;177:169-177.

Simonazzi A, Davies C, Cid AG, Gonzo E, Parada L, Bermudez JM. Preparation and characterization of poloxamer 407 solid dispersions as an alternative strategy to improve benznidazole bioperformance. J Pharm Sci. 2018;107(11):2829-2836.

Soares-Sobrinho JL, de La Roca Soares MF, Lopes PQ, Correia LP, de Souza FS, Macedo RO, et al. A preformulation study of a new medicine for Chagas disease treatment: physicochemical characterization, thermal stability, and compatibility of benznidazole. AAPS PharmSciTech. 2010;11(3):1391-1396.

Soares-Sobrinho JL, Santos FL, Lyra MA, Alves LD, Rolim LA, Lima AA, et al. Benznidazole drug delivery by binary and multicomponent inclusion complexes using cyclodextrins and polymers. Carbohydr Polym. 2012;89(2):323-330.

Soares-Sobrinho JL, Soares MFdLR, Labandeira JJT, Alves LDS, Rolim-Neto PJ. Improving the solubility of the antichagasic drug benznidazole through formation of inclusion complexes with cyclodextrins. Quim Nova. 2011;34(9):1534-1538.

Soeiro MNC, de Souza EM, da Silva CF, Batista DG, Batista MM, Pavao BP, et al. In vitro and in vivo studies of the antiparasitic activity of sterol 14alpha-demethylase (CYP51) inhibitor VNI against drug-resistant strains of Trypanosoma cruzi. Antimicrob Agents Chemother. 2013;57(9):4151-4163.

Streck L, de Araújo MM, de Souza I, Fernandes-Pedrosa MF, do Egito EST, de Oliveira AG, et al. Surfactant–cosurfactant interactions and process parameters involved in the formulation of stable and small droplet-sized benznidazole-loaded soybean O/W emulsions. J Mol Liq. 2014;196:178-186.

Streck L, Sarmento VH, Machado PR, Farias KJ, Fernandes-Pedrosa MF, da Silva-Junior AA. Phase transitions of isotropic to anisotropic biocompatible lipid-based drug delivery systems overcoming insoluble benznidazole loading. Int J Mol Sci. 2016;17(7):981.

Tessarolo LD, de Menezes R, Mello CP, Lima DB, Magalhaes EP, Bezerra EM, et al. Nanoencapsulation of benznidazole in calcium carbonate increases its selectivity to Trypanosoma cruzi. Parasitology. 2018;145(9):1191-1198.

The United States Pharmacopeia and National Formulary (USP39-NF34). Rockville: United States Pharmacopeial Convention; 2016.

Vinuesa T, Herráez R, Oliver L, Elizondo E, Acarregui A, Esquisabel A, et al. Benznidazole nanoformulates: a chance to improve therapeutics for Chagas disease. Am J Trop Med Hyg. 2017;97(5):1469-1476.

Wulff-Perez M, de Vicente J, Martin-Rodriguez A, Galvez-Ruiz MJ. Controlling lipolysis through steric surfactants: new insights on the controlled degradation of submicron emulsions after oral and intravenous administration. Int J Pharm. 2012;423(2):161-166.

Zingales B, Araujo RG, Moreno M, Franco J, Aguiar PH, Nunes SL, et al. A novel ABCG-like transporter of Trypanosoma cruzi is involved in natural resistance to benznidazole. Mem Inst Oswaldo Cruz. 2015;110(3):433-444.

World Health Organization (WHO). Chagas disease (American trypanosomiasis). 2020. Available at: http://www.who.int/chagas/en/.